SCIENCE CHINA
Chemistry

•ARTICLES•

https://doi.org/10.1007/s11426-019-9690-7

In situ formation of fluorescent silicon-containing polymer dots for alkaline phosphatase activity detection and immunoassay

Guoyong Liu[1,2], Jiahui Zhao[1,3], Mengxia Yan[1,2], Shuyun Zhu[1,4], Wenchao Dou[5], Jian Sun[1*] & Xiurong Yang[1,2*]

[1]*State Key Laboratory of Electroanalytical Chemistry, Changchun Institute of Applied Chemistry, Chinese Academy of Sciences, Changchun 130022, China;*
[2]*University of Science and Technology of China, Hefei 230026, China;*
[3]*University of Chinese Academy of Sciences, Beijing 100049, China;*
[4]*College of Chemistry and Chemical Engineering, Qufu Normal University, Qufu 273165, China;*
[5]*Food Safety Key Laboratory of Zhejiang Province, College of Food Science and Biotechnology, Zhejiang Gongshang University, Hangzhou 310018, China*

Received November 27, 2019; accepted January 19, 2020; published online March 12, 2020

The discovery and application of analyte-triggered fluorophore generation or fluorogenic reaction are significant and beneficial to the development of novel fluorescence (FL) analysis method. In this study, for the first time, we have reported a fluorogenic reaction to prepare fluorescent silicon-containing polymer dots (Si-PDs) by simply mixing *N*-[3-(trimethoxysilyl)propyl]ethylenediamine (DAMO) and hydroquinone (HQ) in aqueous solution at ambient temperature. Inspired by the alkaline phosphatase (ALP)-catalyzed hydrolysis of the substrate sodium 4-hydroxyphenyl phosphate (4-HPP) into HQ and the resultant HQ-controlled intense green Si-PDs generation, we have established a straightforward ALP activity assay by innovatively employing commercially available 4-HPP as the substrate. More significantly, the specific preparation method, clear formation mechanism and excellent performance enable the Si-PDs as well as its generation process to develop facile and attractive FL immunoassay. With the help of the universal ALP-based enzyme-linked immunosorbent assay (ELISA) platform and corresponding antibody, a convenient and conceptual ALP-based fluorescent ELISA has been constructed and applied in sensing cardiac troponin I (cTnI), a well-known biomarker of acute myocardial infarction. Our research via *in situ* formation of fluorescent nanomaterials has great potential application in ALP activity assay, inhibitor screening, and disease diagnosis.

fluorescent, polymer dots, ELISA, alkaline phosphatase, cardiac troponin I

Citation: Liu G, Zhao J, Yan M, Zhu S, Dou W, Sun J, Yang X. *In situ* formation of fluorescent silicon-containing polymer dots for alkaline phosphatase activity detection and immunoassay. *Sci China Chem*, 2020, 63, https://doi.org/10.1007/s11426-019-9690-7

1 Introduction

Enzyme-linked immunosorbent assay (ELISA) is extensively employed in laboratory research, food safety control, environmental analysis, clinical diagnosis, and biomedical application [1], owing to its quantification accuracy, easy operation, low cost, and convenient readout. As an important immunoassay format, ELISA mainly depends on the efficient catalytic amplification of enzyme and the specific recognition of antigen-antibody [2]. In typical ELISA, alkaline phosphatase (ALP) acts as one of the most commonly utilized labeling enzymes because of its easy conjugation to antibody, good stability, and high catalytic activity [3–5]. In addition, ALP can hydrolyze numerous phosphorylated substrates, especially phosphate-containing metabolites in an alkaline environment [6]. Abnormal ex-

*Corresponding authors (email: jiansun@ciac.ac.cn; xryang@ciac.ac.cn)

pression of ALP is linked with many diseases, such as hepatobiliary disease and bone disease [7]. Thus, accurate determination of ALP activity is not only beneficial for clinical diagnosis, but also conducive to the development of novel ALP-based ELISA platform.

There have been many analytical approaches for ALP activity detection, such as colorimetry, fluorometry, electrochemistry, chemiluminescence, and surface enhancement Raman scattering [8]. Correspondingly, a number of immunoassays have been established on the basis of these analytical approaches [9]. Among these immunoassays, colorimetry and fluorometry are more popular methods due to their low cost, convenience, simple operation, and easy readout. Nevertheless, conventional colorimetric ELISA is suffering from a high detection limit. The introduction of plasmonic ELISA, a new-type colorimetric immunoassay based on noble metal nanoparticles aggregation, etching, and deposition increases the sensitivity of detection [10,11]. However, noble metal nanoparticles are unstable and are easily interfered by the external environment. In addition, the synthesis or surface modification of nano-sized noble metal particles takes time and effort. As a substitute or supplement for colorimetric immunoassay, fluorescence (FL) immunoassay draws people's attention [12]. In this regard, ALP-based FL immunoassays are mostly established based on the substrate ascorbic acid 2-phosphate (AA2P) [13–17], and *p*-nitrophenyl phosphate (pNPP) [18–20], by means of the high reaction activity of corresponding enzymatic hydrolysates (ascorbic acid and orthophosphate, respectively). And then, exploring new ALP substrates and novel ALP-enabled fluorogenic reaction will undoubtedly enrich and promote the development of FL immunoassays. Recently, our group [21] has synthesized a new ALP substrate, called *m*-hydroxyphenyl phosphate sodium salt (*m*-HPP), but the synthesis process is ineluctably time-consuming and laborious. Therefore, it is necessary and important to construct an efficient, simple, and convenient fluorescent ELISA platform by employing a new commercially available substrate.

Nowadays, fluorescent carbon dots (CDs), mainly including graphene quantum dots (GQDs), carbon nanodots (CNDs), and polymer dots (PDs), have attracted widespread attention due to their superior optical properties, stability, and biocompatibility [22]. A number of approaches for preparing CDs have been developed, such as chemical oxidation, electrochemical etching, hydrothermal or solvothermal synthesis, microwave-assisted synthesis, and so on [23]. At the same time, a variety of heteroatoms (nitrogen, phosphorus, sulfur, boron, silicon, etc.) have been successfully doped into the CDs to modulate their fluorescent properties [24]. However, these synthetic or doping approaches may have to involve hazardous solvents, high temperature and high pressure, and microwave radiation [25]. Here, we try to provide a facile method for preparing fluorescent CDs at room temperature without any external energy supply. It is demonstrated that the fluorescent silicon-containing polymer dots (Si-PDs) can be synthesized in 80 min by simply mixing the solutions of hydroquinone (HQ) and *N*-[3-(trimethoxysilyl)propyl]ethylenediamine (DAMO). The Si-PDs display monodisperse dots with intense green FL, as evidenced by further characterizations. Compared to previous reports, our approach is simple and green, especially can be rapidly completed in aqueous solution at ambient conditions. Such cheap, mild and convenient reaction inspires us to develop an *in situ* approach for biological sample detection.

Herein, we have constructed a simple and convenient fluorescent ELISA based on *in situ* generation of green-emission Si-PDs. The commercially available sodium 4-hydroxyphenyl phosphate (4-HPP) is selected as the ALP substrate. Most significantly, HQ, the enzymatic hydrolysate of 4-HPP, can react with DAMO to form green-emission Si-PDs *in situ*, while 4-HPP hardly reacts with DAMO. The FL intensity directly associates with ALP activity. With the help of the universal ALP-based ELISA platform and corresponding antibody, we construct a novel ALP-based fluorescent ELISA. In an ELISA platform, the concentration of the antigen is related to the ALP-labeled secondary antibody. Thus, the FL intensity can indirectly reflect the concentration of the target antigen. Our approach can be used not only to measure biomarkers with the help of the corresponding antibodies, but also to broaden the potential application of FL nanoparticles.

2 Experimental

2.1 Chemicals

Sodium 4-hydroxyphenyl phosphate (4-HPP) was acquired from Bidepharm Corporation (China). Alkaline phosphatase (ALP), sodium orthovanadate (Na_3VO_4), human serum albumin (HSA), *Eco*R I, trypsin, lysozyme (LZM), glucose oxidase (GOx), and bovine serum albumin (BSA) were supplied by Sigma-Aldrich. Hydroquinone (HQ), Tris-Buffered Saline Tween-20 (TBST), and human immunoglobulin G (IgG) were purchased from Sangon Biotechnology Corporation (China). DAMO was purchased from Aladdin Industrial Corporation (China). Human serum samples were obtained from the Second Hospital of Jilin University (China).

Cardiac troponin T (cTnT), cardiac troponin I (cTnI), mouse anti-cTnI antibody (capture antibody), rabbit anti-cTnI antibody (Ab1), ALP-labeled goat anti-rabbit secondary antibody (ALP-Ab2), carcino-embryonic antigen (CEA), and human alpha-fetoprotein (AFP) were purchased from Abcam Corporation (UK).

2.2 Apparatus

Fluorescence and absorption spectra were carried out on Hitachi F-4600 spectrofluorometer (Japan) and CARY 500 UV-Vis-NIR Varian spectrophotometer (USA), respectively. Transmission electron microscopy (TEM) image was obtained on a Tecnai G2 F20 instrument (FEI, USA). Fourier transform infrared spectroscopy (FTIR) spectra were conducted on a Bruker Optics VERTEX 70 spectrometer (Germany). X-ray diffraction (XRD) pattern and X-ray photoelectron spectroscopy (XPS) measurements were acquired by Bruker D8 ADVANCE and Thermo ESCALAB VG Scientific 250 (UK), respectively.

2.3 Synthesis of fluorescent Si-PDs

100 mg HQ and 5 mL of DAMO were dispersed in 95 mL of deionized water. The resultant solution was allowed to stand at room temperature for 80 min and then lyophilized. The lyophilized crude product was washed thrice with ethanol. The precipitate was collected and dried at room temperature for the further characterization.

2.4 ALP activity measurement

ALP activity was detected as follows. First of all, 180 μL of 50 mM Tris-HCl buffer solution (pH 8.5) containing 50 μM $MgCl_2$, 225 μL of 4-HPP (2.0 mM), 405 μL of water, and 90.0 μL of ALP with different concentrations were mixed and incubated for 60 min at 37 °C. Subsequently, 100 μL of DAMO (50%, *v*/*v*) was added to the mixed solution. Then, the resultant solution was allowed to stand at room temperature for 80 min. Finally, the FL spectrum was recorded with an excitation wavelength of 370 nm. To demonstrate the specificity of our assay, interfering substances (including non-specific enzymes and proteins) were assayed in the presence and absence of ALP.

2.5 FL immunoassay for cTnI

The cTnI detection was carried out by a sandwich format immunoassay procedure. First of all, 100 μL 5 μg/mL of mouse monoclonal antibody in carbonate buffer (100 mM, pH 9.6) was introduced into each well and maintained at 4 °C for 12 h. After discarding the solution, the wells were rinsed three times with TBST, and then blocked with 200 μL 3% BSA for 1 h at 37 °C. Then, the wells were washed thrice with TBST again. Subsequently, 100 μL of cTnI with various concentrations was injected into the wells and maintained for 1 h at 37 °C. The washing steps were repeated. Next, 100 μL 2 μg/mL of Ab1 was added into each well and incubated for 1 h at 37 °C. After washing, 100 μL of ALP-Ab2 (1:5000) was injected into the wells and kept at 37 °C for 1 h, followed by washing again. Afterward, a mixed solution of 45 μL of Tris-HCl buffer solution (pH 8.5, 50 mM) containing 50 μM $MgCl_2$, 56.3 μL of 4-HPP (2.0 mM), and 123.7 μL of water was injected into each well and maintained at 37 °C for 1 h. Subsequently, 25 μL of DAMO (50%, *v*/*v*) was introduced into the wells. After incubation for 80 min at room temperature, FL spectra measurements were performed.

3 Results and discussion

3.1 Characterization of the fluorescent Si-PDs

A previous article had reported a similar reaction that HQ and DAMO could act as precursors to prepare fluorescent nanoparticles. However, the synthesis of fluorescent nanoparticles was carried out at 200 °C for 4 h [26]. To our surprise, we found the fluorescent Si-PDs could be easily synthesized at room temperature in 80 min by simply mixing the aqueous solutions of HQ and DAMO. The optical properties of the as-prepared Si-PDs were studied by absorption and FL spectra. As seen from Figure 1(A), compared with the absorption spectra of DAMO and HQ, the Si-PDs show two new absorption peaks at 370 nm (n-π^* transitions of C=O/C=N) [27] and 500 nm (surface state transitions) [28], respectively. The maximum excitation and emission wavelength of Si-PDs are located at 370 nm and around 520 nm (Figure S1, Supporting Information online), respectively. The Si-PDs solutions display light orange in daylight and strong green FL under the 365 nm UV lamp (inset of Figure 1(A)). The morphology of the Si-PDs was investigated by TEM. The Si-PDs exhibit a spherical structure with a particle size of 20–200 nm (Figure 1(B) and its insert). The XRD pattern shows a broad distinct peak at 20.3° (Figure S2), illustrating that Si-PDs are amorphous nature [29,30]. The TEM image and XRD pattern indicate that Si-PDs are polymer dots (PDs). The surface functional groups of the Si-PDs were studied by FTIR. As shown in Figure 1 (C), compared with the FTIR spectra of DAMO and HQ, the Si-PDs appear a new absorption peak at 1655 cm^{-1}, representing stretching vibration of C=O/C=N [31]. The broad absorption peak around 3400 cm^{-1} is attributed to the stretching vibration of O–H and N–H [32]. The absorption peaks at 2938, 1471, and 1571 cm^{-1} belong to C–H stretching vibration [33], C–H bending vibration [34], and N–H bending vibration [35], respectively. The stretching vibration of C=C, C–N, and C–O can be observed at 1603, 1350, and 1195 cm^{-1}, respectively [36]. The absorption peaks at 1123 and 1034 cm^{-1} can represent stretching vibration of Si–O [37], indicating that silicon has been successfully doped into the polymer dots. To confirm the elemental composition and chemical bonding of the Si-PDs, XPS measurements were carried out. As seen from Figure 1(D), the Si-PDs contain

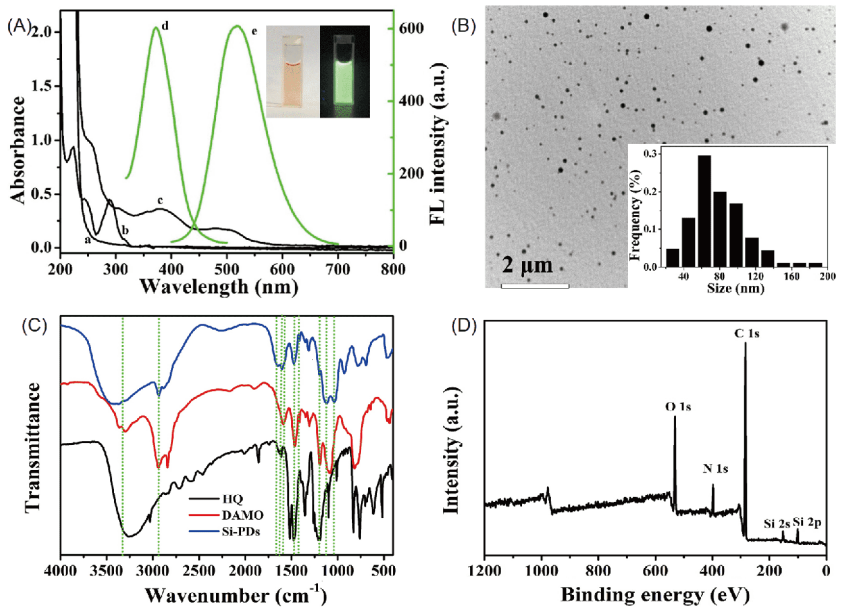

Figure 1 (A) Absorption spectra of DAMO (a), HQ (b), and Si-PDs (c), and the maximum excitation (d) and emission (e) spectra of Si-PDs. Insets are optical photographs of Si-PDs solutions in daylight (left) and 365 nm UV light (right). (B) TEM image of Si-PDs. Inset is the distribution histogram of particle size. (C) FTIR spectra of HQ (black), DAMO (red), and Si-PDs (blue). (D) The full survey of the XPS spectrum of Si-PDs (color online).

four non-hydrogen elements of C (284 eV), N (398 eV), O (531 eV), and Si (102 and 152 eV) [38]. The spectra of C 1s, N 1s, O 1s, and Si 2p are shown in Figure S3. The C 1s spectrum is divided into four parts at 284.0, 284.6, 285.7, and 288.5 eV, which can be associated with C–Si, C–C/C=C, C–O/C–N, and C=O/C=N bonds, respectively [39]. The N 1s spectrum displays three peaks located at 398.3, 399.0, and 400.1 eV, corresponding to C=N/N–Si, C–N, and N–H bonds, respectively [40,41]. O–Si (531.0 eV), C–O (531.9 eV), and C=O (533.4 eV) bonds can be seen from O 1s spectrum [42]. The Si 2p spectrum implies the existence of Si–C (101.0 eV), Si–N (101.6 eV), and Si–O (102.2 eV) bonds, respectively [43]. The results of XPS characterization are consistent with those of FTIR characterization. The comprehensive characterization results indicate that we have successfully synthesized fluorescent Si-PDs with abundant functional groups on the surface.

3.2 Establishment and optimization of ALP sensing system

To obtain favorable sensing performance, the reaction parameters of HQ and DAMO were optimized. As illustrated in Figure S4, as the DAMO concentration and reaction time increase, the FL intensities at 520 nm of the Si-PDs also increase. To save reagents and time, the DAMO concentration and reaction time were chosen to be 5% and 80 min, respectively. When the concentration of DAMO and reaction time were fixed, we studied the relationship between HQ concentration and FL intensity in detail. As presented in Figure 2(a, b), the FL intensity at 520 nm exhibits concentration-dependent increase with increasing HQ concentration. A good linearity (R^2=0.992) between the concentration of HQ (1 to 80 μM) and FL intensity can be obtained, indicating that we may monitor HQ-related targets. In this regard, HQ could be considered as the dephosphorylated enzymatic product of 4-HPP through ALP-catalyzed cleavage of the phosphoester bond in 4-HPP. To verify the feasibility of 4-HPP as a substrate for ALP, we performed absorption and FL spectra measurements. As depicted in Figure 3(B, C), 4-HPP solution (line a), the mixed solution of 4-HPP and DAMO (line b), and the mixed solution of ALP and DAMO (line c) display no absorption peak at 370 nm and FL signal at 520 nm. The mixed solution of 4-HPP and ALP (line d) has an absorption peak at 350 nm, but no FL signal at 520 nm. The mixed solution of 4-HPP and ALP after adding DAMO (line e) shows two characteristic absorption peaks at 370 and 500 nm. Meanwhile, a FL signal at 520 nm can be observed in the FL spectra. The absorption and FL spectra of *in situ* formation of products catalyzed by ALP coincide with those of as-prepared Si-PDs (line f). Thus, 4-HPP can be used as the substrate for ALP activity sensing based on the ALP-enabled produce of FL signal (Figure 3(A)).

To acquire optimal sensing performance, we investigated the experimental parameters in the presence and absence of ALP. As shown in Figure S5, in the absence of ALP, the background signals (red bar) are negligible. Meanwhile, in the presence of ALP, the favorable conditions of the pH, the 4-HPP concentration, the incubation time of ALP, and

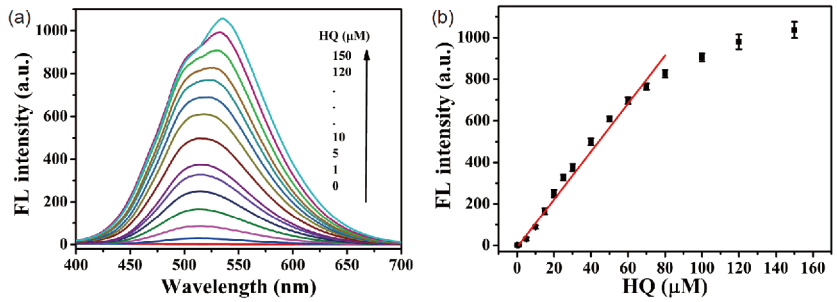

Figure 2 FL emission spectra (a) and corresponding FL intensities (b) of HQ with various concentrations in the presence of 5% (*v*/*v*) DAMO (color online).

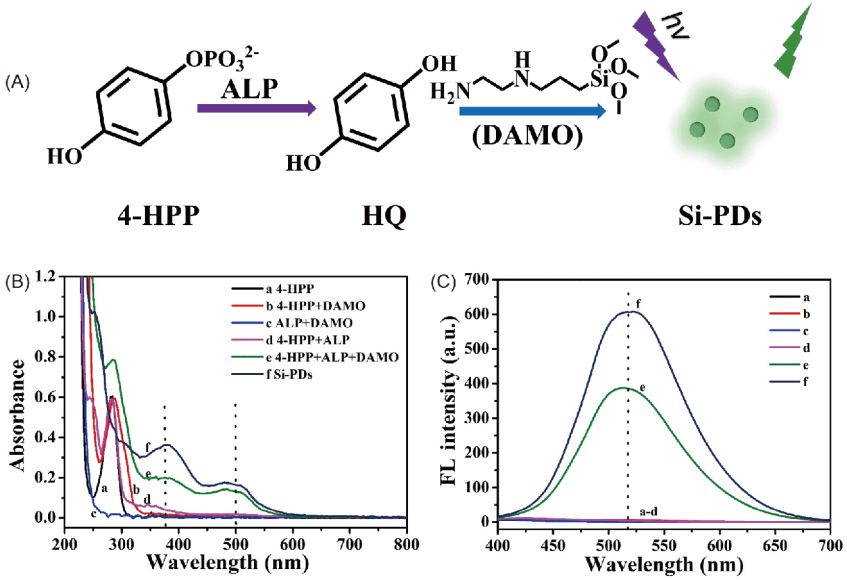

Figure 3 (A) Principle of ALP-catalyzed *in situ* generation of Si-PDs. (B) Absorption and (C) FL emission spectra of 4-HPP (a), 4-HPP+DAMO (b), ALP +DAMO (c), 4-HPP+ALP (d), 4-HPP+ALP+DAMO (e), as-prepared Si-PDs (f). The concentrations of 4-HPP, DAMO, and ALP are 0.5 mM, 5%, and 20 mU/mL, respectively. The Si-PDs are prepared by reaction of HQ (50 μM) and DAMO (5%) at room temperature for 80 min (color online).

the fluorogenic reaction time of ALP-incubated 4-HPP with DAMO are 8.5, 0.5 mM, 60 min, and 80 min, respectively.

3.3 FL assay for ALP activity and its inhibitor

Under optimal experimental conditions, the relationship between ALP concentration and FL intensity was investigated in detail. As presented in Figure 4(a), as the ALP concentration increases, the FL intensity of the sensing system increases gradually. ALP concentrations between 0.7 and 50 mU/mL have a good linear relationship (R^2=0.996) with FL intensities at 520 nm (F_1), as depicted in Figure 4(b). The linear relationship can be express as F_1=19.12C_{ALP}–4.25. The limit of detection is 0.1 mU/mL, which is lower than the previously reported assays for ALP (Table S1, Supporting Information online). Using non-specific proteins and enzymes as controls, we investigated the selectivity of the assay. As indicated in Figure S6, in the presence of ALP, the effects of interfering substances can be neglected. In the absence of ALP, the interfering substances cannot produce FL signals. These results demonstrate the good selectivity of the assay for ALP detection.

Inhibitor studies of enzymes have an important impact on drug design/discovery. By using a common ALP inhibitor (Na_3VO_4), the proposed assay was utilized to assess the efficiency of enzyme inhibitor.

As the concentrations of Na_3VO_4 increase from 1 to 1,500 μM, the ALP activity (20 mU/mL) is gradually suppressed, resulting in a decrease in the FL intensity of the test solution (Figure S7(a)). There is a sigmoidal curve relationship between the FL intensities and the logarithm of Na_3VO_4 concentrations (Figure S7(b)). The IC_{50} value (the concentration of an inhibitor that is required for 50% inhibition of enzyme activity) is approximately 25.9 μM. This value is consistent with previously reported value [44], indicating that our assay could be utilized for the screening of ALP inhibitor.

3.4 ALP-based fluorescent ELISA for cTnI detection

Encouraged by the good results of ALP detection and the widespread use of ELISA, we attempted to develop a novel ALP-based fluorescent ELISA for the determination of antigens. cTnI, a biomarker of acute myocardial infarction (AMI), is chosen as a model. When AMI occurs, the cTnI concentration increases, even reaching to 550 ng/mL or above. Thus, accurate determination of cTnI concentration is of great significance in the early diagnosis of AMI [45]. With the help of commercial antibodies to cTnI, we investigated the ability of our proposed fluorescent ELISA to detect cTnI. Figure 5(a) schematically depicts the fluorescent ELISA for cTnI detection via ALP-catalyzed *in situ* generation of Si-PDs. In this strategy, the capture antibody is first immunized to the well. The cTnI is then captured by the capture antibody. Subsequently, the Ab1 recognizes the cTnI and the Ab2 recognizes the Ab1, resulting in the formation of a sandwiched immunocomplex. ALP connected to the Ab2 catalyzes the hydrolysis of 4-HPP to form HQ, which could react with DAMO to produce intense green-emission Si-PDs *in situ*. Therefore, the FL intensity establishes an indirect relationship with the cTnI concentration. As shown in Figure 5(b, c), the FL intensities exhibit a concentration-dependent increase with the increase of cTnI concentration. This relationship between FL intensities (F_2) and cTnI concentrations (1–300 ng/mL) can be expressed as F_2=9.06+0.77C_{cTnI}, R^2=0.997. Compared with previously reported immunoassays for cTnI (Table S2), a comparable detection limit of 0.1 ng/mL is obtained. To verify the selectivity of the immunoassay for cTnI, some non-specific proteins, including cTnT, trypsin, IgG, CEA, LZM, and AFP, were chosen as controls. The effects of various interfering substances on the sensing system are negligible, as depicted in Figure 5(d). The above results demonstrate that our fluorescent ELISA exhibits excellent sensitivity and specificity for cTnI. Fur-

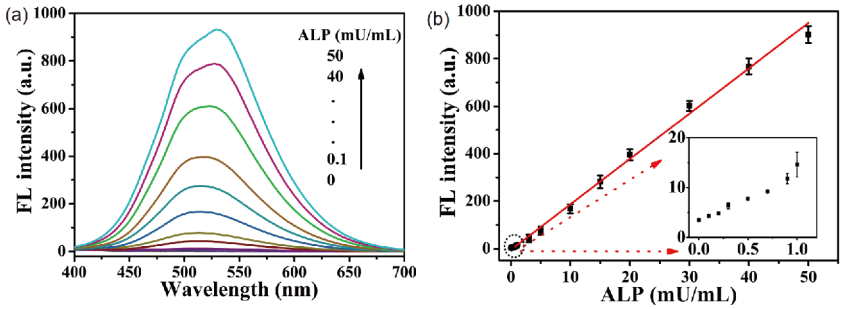

Figure 4 (a) FL emission spectra and (b) the corresponding FL intensities of Si-PDs formed by *in situ* catalysis of ALP with different concentrations (color online).

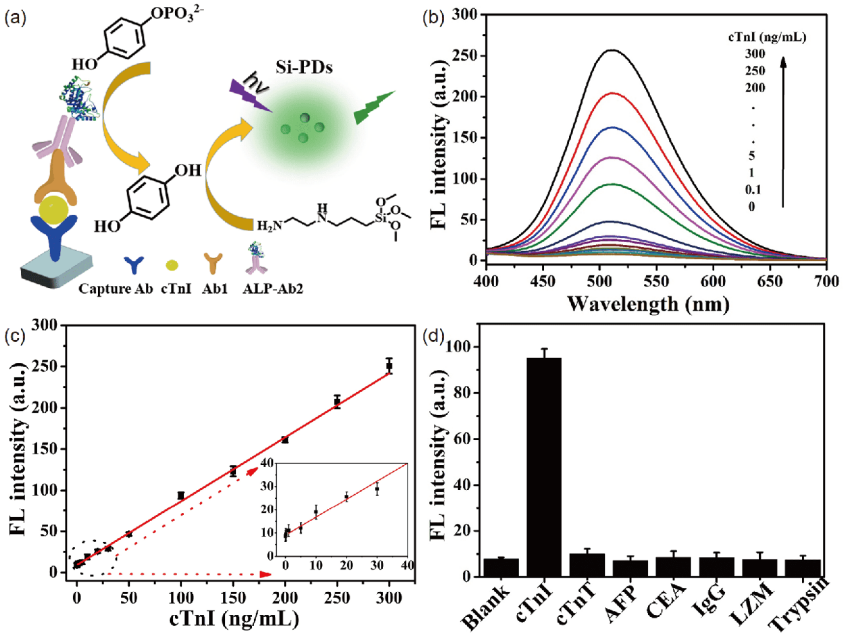

Figure 5 (a) Schematic illustration of the fluorescent ELISA. (b) The FL emission spectra and (c) the corresponding FL intensities of the fluorescent ELISA in the presence of various concentrations of cTnI (inset: the linear relationship from 1 to 30 ng/mL). (d) Selectivity investigation of the fluorescent ELISA for cTnI. The cTnI and other proteins/enzymes are 100 ng/mL (color online).

thermore, we employed a conventional colorimetric pNPP-based standard ELISA kit and our proposed FL ELISA to detect cTnI in spiked human serum samples, respectively. As presented in Figure S8, the results of the conventional colorimetric ELISA are in good agreement with those of our developed fluorescent ELISA, indicating that our fluorescent ELISA has great potential for cTnI detection in real samples.

4 Conclusions

In summary, we provide a facile method for preparing strong green-emission Si-PDs at room temperature by simply mixing the solutions of HQ and DAMO. Owing to the ALP-catalyzed specific conversion of 4-HPP into HQ and the difference in the reaction with DAMO between HQ and 4-HPP, we develop a simple strategy to detect ALP activity and its inhibitor based on *in situ* formation of green-emission Si-PDs. Inspired by the widespread use of ELISA and ALP-catalyzed *in situ* generation of green-emission Si-PDs, we have constructed a novel fluorescent ELISA for cTnI detection. The results of the proposed fluorescent ELISA for cTnI detection in diluted human serum coincide with those of standard colorimetric ELISA. Under the unambiguously recognition mechanism and easy signal generation approach, our research has great potential application in ALP activity assay, inhibitor screening, and disease diagnosis.

Acknowledgements This work was supported by the National Key Research and Development Program of China (2016YFA0201301), the National Natural Science Foundation of China (21435005, 21627808, 21974132), the Youth Innovation Promotion Association, CAS (2018258) and Open Project of State Key Laboratory of Supramolecular Structure and Materials (sklssm2019023).

Conflict of interest The authors declare that they have no conflict of interest.

Supporting information The supporting information is available online at http://chem.scichina.com and http://link.springer.com/journal/11426. The supporting materials are published as submitted, without typesetting or editing. The responsibility for scientific accuracy and content remains entirely with the authors.

1 Shen J, Li Y, Gu H, Xia F, Zuo X. *Chem Rev*, 2014, 114: 7631–7677
2 de la Rica R, Stevens MM. *Nat Protoc*, 2013, 8: 1759–1764
3 Liu Y, Pan M, Wang W, Jiang Q, Wang F, Pang DW, Liu X. *Anal Chem*, 2019, 91: 2086–2092
4 Chen Z, Wang H, Zhang Z, Chen L. *Anal Chem*, 2019, 91: 1254–1259
5 Gao Z, Deng K, Wang XD, Miró M, Tang D. *ACS Appl Mater Interfaces*, 2014, 6: 18243–18250
6 Millán JL. *Purinergic Signalling*, 2006, 2: 335–341
7 Fernandez NJ, Kidney BA. *Vet Clin Pathol*, 2007, 36: 223–233
8 Tang Z, Chen H, He H, Ma C. *TrAC Trends Anal Chem*, 2019, 113: 32–43
9 Fu X, Chen L, Choo J. *Anal Chem*, 2017, 89: 124–137
10 Ma X, He S, Qiu B, Luo F, Guo L, Lin Z. *ACS Sens*, 2019, 4: 782–791
11 Tang L, Li J. *ACS Sens*, 2017, 2: 857–875
12 Guo Y, Zhao W. *Coordin Chem Rev*, 2019, 387: 249–261
13 Hu XL, Wu XM, Fang X, Li ZJ, Wang GL. *Biosens Bioelectron*, 2016, 77: 666–672
14 Sun J, Hu T, Chen C, Zhao D, Yang F, Yang X. *Anal Chem*, 2016, 88: 9789–9795
15 Sun J, Hu T, Xu X, Wang L, Yang X. *Nanoscale*, 2016, 8: 16846–16850
16 Yuan Y, Wu W, Xu S, Liu B. *Chem Commun*, 2017, 53: 5287–5290
17 Zhao D, Li J, Peng C, Zhu S, Sun J, Yang X. *Anal Chem*, 2019, 91: 2978–2984
18 Chen C, Zhao J, Lu Y, Sun J, Yang X. *Anal Chem*, 2018, 90: 3505–3511
19 Malashikhina N, Garai-Ibabe G, Pavlov V. *Anal Chem*, 2013, 85: 6866–6870
20 Grinyte R, Barroso J, Möller M, Saa L, Pavlov V. *ACS Appl Mater Interfaces*, 2016, 8: 29252–29260
21 Zhao J, Wang S, Lu S, Liu G, Sun J, Yang X. *Anal Chem*, 2019, 91: 7828–7834
22 Zhu S, Song Y, Zhao X, Shao J, Zhang J, Yang B. *Nano Res*, 2015, 8: 355–381
23 Liu ML, Chen BB, Li CM, Huang CZ. *Sci China Chem*, 2019, 62: 968–981
24 Zhou J, Zhou H, Tang J, Deng S, Yan F, Li W, Qu M. *Microchim Acta*, 2016, 184: 343–368
25 Liu ML, Chen BB, Li CM, Huang CZ. *Green Chem*, 2019, 21: 449–471
26 Liu Y, Wang Q, Guo S, Jia P, Shui Y, Yao S, Huang C, Zhang M, Wang L. *Sens Actuat B-Chem*, 2018, 275: 415–421
27 Han L, Liu SG, Dong JX, Liang JY, Li LJ, Li NB, Luo HQ. *J Mater Chem C*, 2017, 5: 10785–10793
28 Zhu S, Shao J, Song Y, Zhao X, Du J, Wang L, Wang H, Zhang K, Zhang J, Yang B. *Nanoscale*, 2015, 7: 7927–7933
29 Zheng J, Wang Y, Zhang F, Yang Y, Liu X, Guo K, Wang H, Xu B. *J Mater Chem C*, 2017, 5: 8105–8111
30 Wang D, Wang X, Xu C, Ma X. *Sci China Chem*, 2019, 62: 430–433
31 Chen BB, Liu ZX, Deng WC, Zhan L, Liu ML, Huang CZ. *Green Chem*, 2016, 18: 5127–5132
32 Liu Z, Zou H, Wang N, Yang T, Peng Z, Wang J, Li N, Huang C. *Sci China Chem*, 2018, 61: 490–496
33 Zhang T, Zhu J, Zhai Y, Wang H, Bai X, Dong B, Wang H, Song H. *Nanoscale*, 2017, 9: 13042–13051
34 Purkait TK, Iqbal M, Islam MA, Mobarok MH, Gonzalez CM, Hadidi L, Veinot JGC. *J Am Chem Soc*, 2016, 138: 7114–7120
35 Li D, Jing P, Sun L, An Y, Shan X, Lu X, Zhou D, Han D, Shen D, Zhai Y, Qu S, Zbořil R, Rogach AL. *Adv Mater*, 2018, 30: 1705913
36 Sun S, Zhang L, Jiang K, Wu A, Lin H. *Chem Mater*, 2016, 28: 8659–8668
37 Han Y, Chen Y, Feng J, Liu J, Ma S, Chen X. *Anal Chem*, 2017, 89: 3001–3008
38 Arslan O, Aytac Z, Uyar T. *J Mater Chem C*, 2017, 5: 1816–1825
39 Ma SD, Chen YL, Feng J, Liu JJ, Zuo XW, Chen XG. *Anal Chem*, 2016, 88: 10474–10481
40 Geng X, Li Z, Hu Y, Liu H, Sun Y, Meng H, Wang Y, Qu L, Lin Y. *ACS Appl Mater Interfaces*, 2018, 10: 27979–27986
41 Lu S, Sui L, Liu J, Zhu S, Chen A, Jin M, Yang B. *Adv Mater*, 2017, 29: 1603443
42 Li Y, Li W, Zhang H, Dong R, Li D, Liu Y, Huang L, Lei B. *J Mater Chem B*, 2019, 7: 1107–1115
43 Han Y, Chen Y, Liu J, Niu X, Ma Y, Ma S, Chen X. *Sens Actuat B-Chem*, 2018, 263: 508–516
44 Guo Z, Zhu X, Wang S, Lei C, Huang Y, Nie Z, Yao S. *Nanoscale*, 2018, 10: 19579–19585
45 Han X, Li S, Peng Z, Othman AM, Leblanc R. *ACS Sens*, 2016, 1: 106–114